Flood retention lakes in a rural-urban catchment: how can they be better used for flood mitigation?

Haochen Yan[1], Mingfu Guan[1,2*] , Yong Kong[1]

[1]Department of Civil Engineering, The University of Hong Kong, Hong Kong SAR, China

[2]The University of Hong Kong Shenzhen Institute of Research and Innovation, Shenzhen, China

Corresponding author: Mingfu Guan (mfguan@hku.hk)

Key Points:

- Flood retention lakes interact with the river channel through 4 typical stages that finally projects catchment-scale performances
- Climate-controlled performances of the retention lake is satisfactory within an L-shaped band in the frequency-duration diagram
- Distributed and parallel configurations yield greater benefits to mitigate maximum inundation; downstream controls suit moderate events

Abstract

Flood retention lakes (RLs) are widely employed in rural-urban catchments with low impacts on the natural environment. While hydrologic models have been commonly applied to evaluate RLs' performances, insights are lacking over the consequences of a wide climatic variability, particularly those corroborated by 2D hydrodynamic models. Thus, this study aims to conduct a systematic catchment-scale evaluation of RL effectiveness; blueprinted RLs with various geographic configurations are also considered in addition to the individual RL. A 2D hydrodynamic model is verified to be capable of simulating flood events in the rural-urban catchment interacted with RLs. Under a wide range (1- to 15- hour duration and 1- to 100-year return period) of rainstorm scenarios, the RL has a satisfactory performance within an L-shaped band in the frequency-duration diagram. The L-shaped band coincides with moderate return periods (10- to 25- year) and large durations (> 6 hours) or small durations (< 4 hours) and large return periods (> 25-year), whereas different criteria yield different optimal combinations. With the increase of event size, 4 typical stages of RL-river interactions are characterized, which projects the catchment-scale performances. Blueprinted RLs with distributed and parallel connections mitigate larger areas of inundation in sub-watersheds than aggregated and series ones. Upstream controls are less effective than downstream controls under moderate events while the relation is reversed for extreme events. Critical changing factors concerning RL-river interactions and spatiotemporal rainstorm variabilities prompt comprehensive considerations of both local-scale RL configurations and catchment-scale climate characterizations.

1 Introduction

Hydro-meteorological extremes are projected to increase in both frequency and intensity owing to global warming (IPCC, 2021). As population and economic assets increase particularly in rural and urban areas, flood exposure and associated damages are expected to rise consequently (Tellman et al., 2021), with both coastal and riverine cities bearing the brunt (Hallegatte et al., 2013; Lai et al., 2020; Mård et al., 2018). The lag between the pace of urbanization and upgrade of flood protection level especially in emerging cities makes the situation even more pressing (Merz et al., 2021; Tellman et al., 2021). Hence, timely and effective stormwater measures are essential to enhance social resilience to climate threats and improve human well-being (Maragno et al., 2018; Ruangpan et al., 2020). Nature-Based Solutions (NBSs) have been widely considered to be capable of effectively addressing environmental challenges and simultaneously providing biodiversity benefits (Cohen-Shacham et al., 2016; Qin et al., 2013) by taking actions that are inspired, supported or copied from nature (European Commission, 2015). Flood retention lake (RL) (or retention basin), a common type of NBSs, typically intercepts part of runoff during flooding events and keeps for subsequent release (Yang et al., 2011). Their capabilities of reducing downstream runoff and damping the flood peak generally decline with the increase of event magnitude but vary dramatically for different cases (Ayalew et al., 2015; Bellu et al., 2016; Birkinshaw et al., 2021; Chen et al., 2007). In fact, a quantitative effectiveness evaluation of RLs remains a challenging issue not only due to methodological limitations, but also its complex sensitivity to climatic factors as well as catchment characteristics including RL configurations.

Methods to evaluate the effects of RLs on catchment hydrology can be generally classified into data-driven and model-driven categories. Data-driven methods perform statistical analysis on a mass of field measurements taken at locations that RLs potentially affect, which can be

compared to the sites with similar landcover and climates (Loperfido et al., 2014), or the same site in pre-construction periods (Birkinshaw et al., 2021). However, the applicability maybe entangled by disparities and changes of the land cover and the climate, also limited by data quality and quantity (Habets et al., 2018). Model-driven methods can provide robust supplementary particularly for data scarce sites/scenarios. Hydrologic models, sometimes combined with 1D hydrodynamic models, have been extensively applied to efficiently and efficaciously simulate rural and urban stormwater systems (Ayalew et al., 2015; Jato-Espino et al., 2019; Lim & Welty, 2017; Luan et al., 2019). However, they are built upon simplifications in sub-catchment definition (preset demarcations for hydrologic units), process calculation (without or over-simplified momentum equations) and results presentation (aggregated and localized quantities). By comparison, hydrodynamic models particularly based on shallow water equations (SWEs) can achieve more realistic simulations, particularly for large events, as they can reproduce the dynamics rainfall-runoff process both spatially and temporally, with much fewer empirical parameters to be calibrated (Bates et al., 2010; Guo et al., 2021; Ming et al., 2020). Being extended to rural and urban flash flood modeling (Bellu et al., 2016; Guo et al., 2021; He et al., 2021; Xia et al., 2017), they have demonstrated promising capabilities for further applications (including both near-field hydraulics and far-field rainfall-runoff processes) on the catchment-scale evaluation of RL performances.

Climate factors dominating floods fundamentally can be considered through intensity, duration, and the total amount of rainstorm events. It is commonly perceived and also verified that peak runoff and runoff depth increase with rainfall intensity and rainfall amount (Miller et al., 2021); longer duration storms tend to cause an increasing amount of rainfall (Lai et al., 2020), while events with time scales comparable with catchment response time scale are likely to produce extreme floods. Guan et al. (2015a, 2015b) found that the ratio of runoff depth to rainfall depth almost remains constant for small events while it increases with considerable fluctuations as rainfall depth exceeds a threshold, due to the effect of intensity and duration. With the existence of RLs, the downstream peak runoff is projected to decrease in most studies with declining effectiveness as the increase of event size, but relatively less attention is paid to event durations (Ayalew et al., 2015; Birkinshaw et al., 2021; Chen et al., 2007; Vojinovic et al., 2021). While recent evidence indicates short-duration events are favored to achieve a better RL performance (Bellu et al., 2016), further investigations are needed by jointly considering events exceeding probability and duration with well-defined event processes guided by systematic frequency analysis.

In addition to climate factors, configurations of RLs also dominate the characteristics of catchment response, including the number and capacity of RLs and spatial placement. The combined effects of a group of RLs, and/or their interplay with other grey/green infrastructures can significantly differ from the simple summation of individuals, owing to the nonlinearity of the catchment system in terms of flood routing, as well as the nonlinear relation between the effectiveness of individual infrastructures and size of implementation (Luan et al., 2019). It is found that dispersed or distributed layouts yield better effectiveness than centralized or aggregated layouts assisted by a cellular model (Zellner et al., 2016), consistent with a data-driven comparative study carried out by Loperfido et al. (2014). Alongside this, RLs placed in parallel or upstream sections of the catchment have better flood control than those placed in series or near the downstream outlet demonstrated by a hydrologic model-based study (Ayalew et al., 2015). Analytical models developed by Del Giudice et al. (2014a, 2014b) based on linear reservoir assumptions indicate that the overall effectiveness of parallel-connected RLs is the sum

of each one while that of series connection is a complex function of RLs and upstream watershed characteristics and may lead to negative effects with additional RLs. Besides, RLs placed closer to upstream contribute to a higher overall efficacy due to a larger ratio of RL size to effective drainage area. Nevertheless, little is known about climate controls (e.g., event size) on various spatial configurations; evidence and insights furnished by hydrodynamic models are still lacking.

Given the points identified above, this study seeks to provide further insights into hydrological and hydraulic responses of RLs with various geographical configurations in rural-urban catchments and a referrable framework for the optimal design of RLs as well as a wider scope of NBSs. Specifically, following questions are to be elaborated:

(1) How do hydrodynamic interactions between a flood retention lake and river channel affect catchment-scale hydrologic response in floods?

(2) What is the typical performance of a RL under a wide range of rainfall scenarios?

(3) How do different geographic configurations of blueprinted RLs influence their effectiveness?

2 Study site and data

This study is primarily enlightened by the recently constructed flood retention lake (RL) located at the upstream reach of the Shenzhen River (ERM Hong Kong, 2010), which is the boundary river between the Hong Kong Special Administration Region (HKSAR) and the Shenzhen Special Economic Zone, China. The entire Shenzhen River flows from east to west into the Shen Zhen Bay, with a length of 37.6 km and basin area of 312.5 km^2 (the ratio between the area of Shenzhen and Hong Kong sides is about 1.5). The basin is governed by subtropical climate, with a mean annual precipitation of about 1606 mm, susceptible to typhoons and low-pressure troughs that frequently induce extreme rainfalls and storm surges (Peking University, 2016). The upper reach of the Shenzhen River (upstream of the confluence point with the Ping Yuen River) is generally narrow and winding with uneven width and collapsed embankment. Similar to the entire Shenzhen River Basin, the Shenzhen side of the basin is highly urbanized while the Hong Kong side is mainly rural (belonging to the North Territory), as shown in Fig. 1. To upgrade the flood protection standard (flood prevention capacity from the range of 2-year to 20-year return period to 20-year to 50-year return period), the Stage-4 River Regulation Project has been conducted during 2012-2017, starting from the confluence point, passing through the Liantang / Heung Yuen Wai Boundary Control Point, ending at about 4.5 km upstream near Pak Fu Shan in Hong Kong (ERM Hong Kong, 2010). The project consisted of (1) river channel modification using a trapezoid compound channel that in principle follows the original watercourse and maintain the naturalness of the river and riparian habitats; (2) a flood retention lake (RL) covering and area of 22000 m^2 with a storage capacity of about 80000 m^3 and overflow weirs will be used in the inlet and outlet of the RL (ERM Hong Kong, 2010). While the project also has comprehensive ecological considerations, this study mainly takes the hydrological perspective and is not limited to the current configurations.

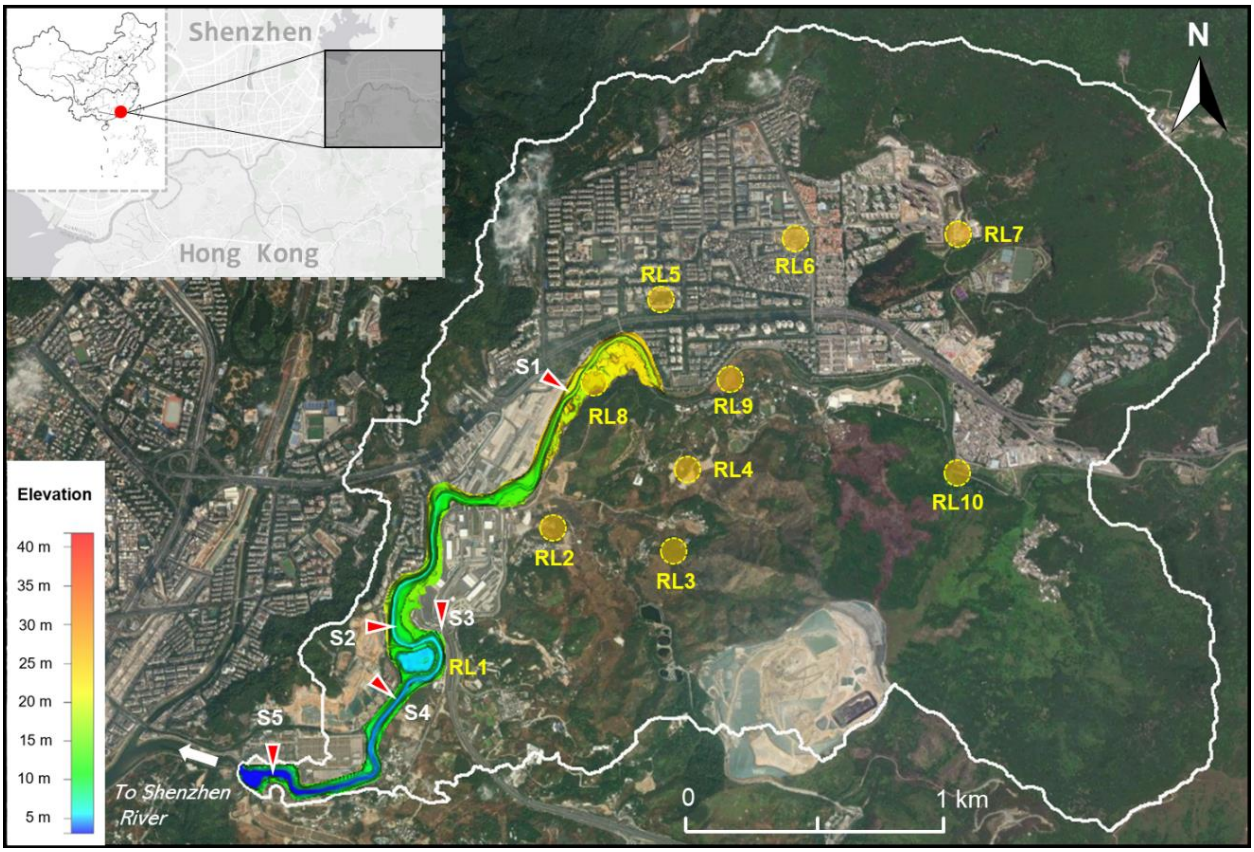

Fig. 1 The upstream catchment of the Shenzhen River Basin. With the satellite image showing land use conditions, only the DEM of the floodplain modified by the Shenzhen River Regulation Stage-4 project is shown. RL1 is the flood retention lake constructed in the project, RL2 to RL10 are potential RL sites considered in this study. S1 is the Liangtang hydrologic station, S2 and S4 are respectively the near upstream and downstream locations of the RL, S3 is the outlet of a tributary at Hong Kong side, S5 is the downstream outlet of the catchment.

The data used in this study (Table 1) mainly include hydrological and geographic aspects. Long-term (1986-2020) hourly rainfall at Ta Ku Ling station (about 2 km from the pond) was obtained from Hong Kong Observatory, based on which the frequency analysis is carried out. In addition, the 2.5-year local hydrologic data from June 2018 to December 2020 measured at Liantang station (about 1km upstream from the RL) with varying temporal resolution from minutes to hours, including runoff and local rainfall used for event-based model calibration and validation, were obtained from the Shenzhen River Regulation Office of Water Authority of Shenzhen Municipality. The as-built river bathymetry of the regulation project in a form of survey points was also provided by the same department, which was then interpolated (presented in Fig. 1) and combined with satellite-derived Digital Elevation Model (DEM) of the entire studied basin, with a 2-m spatial resolution. The land use data of the basin, which are necessary for the assignment of surface roughness and infiltration properties, were manually delineated from the Google satellite image and processed to have the same resolution as the DEM. To evaluate the effectiveness of current RL, the DEM without the RL is produced by filling the RL with the same elevation with the surrounding bank; to study the effect of blueprinted RLs with various geographic configurations, potential RLs sites (marked in Fig. 1) are selected according

to the DEM as well as the land use conditions, which will be interpreted in greater details in the next section.

Table 1 Data list with their source and purpose in this study

Data	Source	Purpose
Rainfall at Liantang station 2018 - 2020	Shenzhen River Regulation Office	Model calibration and validation
Runoff at Liantang station 2018 - 2020	Shenzhen River Regulation Office	
Rainfall at Ta Ku Ling station 1986 - 2020	Hong Kong Observatory	Frequency analysis and event design
2m resolution DEM of the Shenzhen River Basin	ZY-3 Satellite image	Derive the terrain model of the 2D simulation domain
Elevation survey of the river channel	Shenzhen River Regulation Office	Refine the terrain model within the region of river channel
Land use conditions of 2020	Google Earth	Assignment of infiltration and surface roughness properties

3 Methods

3.1 Hydrodynamic modeling

In this study, the unsteady free surface flow of rainfall-runoff process is modeled by solving the full 2D shallow water equations (SWEs) (Brunner, 2021):

$$\frac{\partial h}{\partial t} + \boldsymbol{\nabla} \cdot (h\boldsymbol{V}) = q \quad (1)$$

$$\frac{\partial \boldsymbol{V}}{\partial t} + (\boldsymbol{V} \cdot \boldsymbol{\nabla})\boldsymbol{V} = -g\boldsymbol{\nabla} z_s + \frac{1}{h}\boldsymbol{\nabla} \cdot (\boldsymbol{\nu_t} h \boldsymbol{\nabla V}) - \frac{\boldsymbol{\tau_b}}{\rho R} \quad (2)$$

where h = water depth (L), $\boldsymbol{V}$ = horizontal velocity vector (L/T), z_s = water surface elevation (L), g = gravitational acceleration (L/T^2), $q = I_R + I_I$ = source/sink flux term (L/T), in which I_R and I_I are rainfall intensity and infiltration rate respectively, ρ = density of water (M/L^3), R = hydraulic radius (L), $\boldsymbol{\tau_b} = \rho \frac{n^2 g}{R^{1/3}} |\boldsymbol{V}| \boldsymbol{V}$ = bottom shear stress (M/L/T^2) and n is Manning's roughness coefficient (s/m$^{1/3}$). Infiltration is modeled by the Green-Amt method assuming a saturated condition is already established before each rainfall event for a conservative consideration, although it is proved by preliminary runs to be secondary compared to rainfall for events with time a scale of a few hours.

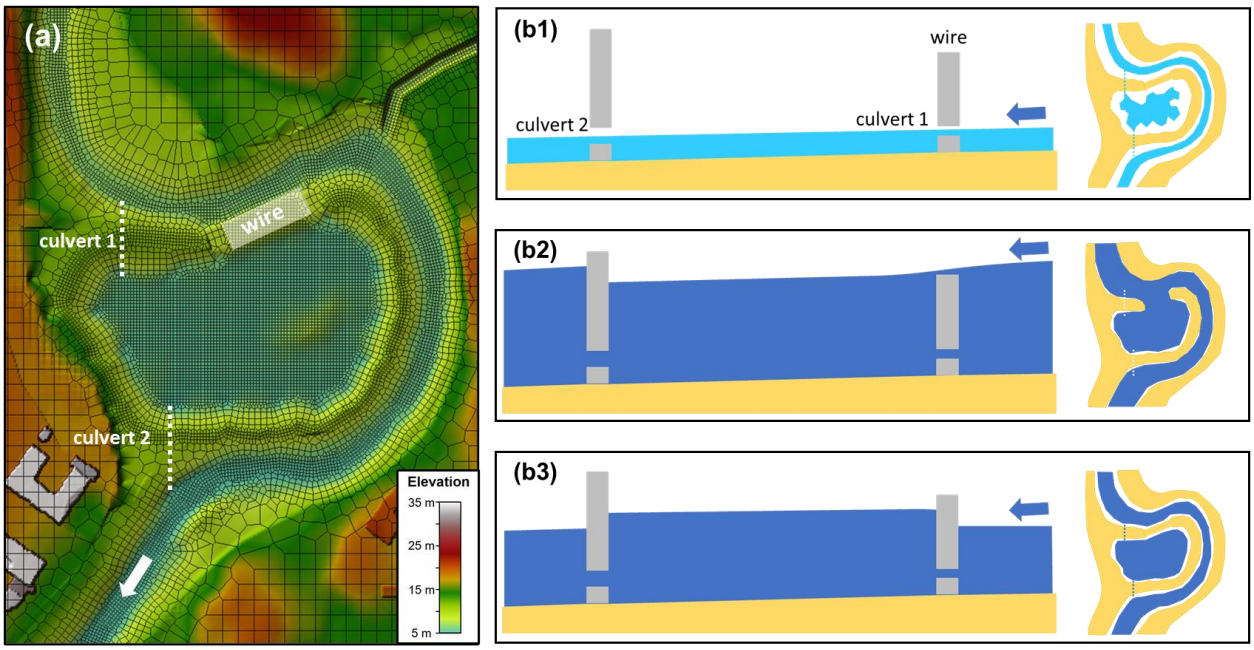

Fig. 2 Computational meshes zoomed-in to the RL (a) and schematic functions of the RL before (b1), during (b2) and shortly after (b3) a flood event.

The numerical simulation is driven by HEC-RAS 6.0 (Brunner, 2021), which is a widely used and free software for 1D, 2D or combined natural or constructed river systems modeling. Recently it has also been applied to urban flood inundation modeling and demonstrated decent performance (David & Schmalz, 2020; Zeiger & Hubbart, 2021). Unstructured polygon meshes are generated for the simulation domain, where full 2D SWEs are solved by the Eulerian-Lagrangian scheme. In this study, 10-m uniform meshes are first established for the entire basin, refinement areas including floodplains and retention lakes are then delineated to have a mesh size of about 2 m (Fig. 2a). The total number of meshes is about 20k, with an average cell size of 72 m^2. Besides the entire 2D domain, 2 culverts are added at upstream and downstream banks of the RL to connect the RL with the main channel at a lower elevation compared to the long broad wire (Fig. 2a). Therefore, water can freely enter and exit the RL under low-flow condition to maintain an aquifer environment and release the impounded water after floods (Fig. 2 b1&b3). During flood condition (Fig. 2 b2), a great majority of water flows into the RL through the long broad wire while that flows across the culverts are nominal due to the small water elevation difference as well as the small diameters (0.3 m for upstream culvert and 0.5 m for downstream culvert). While this setting is only an assumption that mimics the real situation of human control, the effect is very close to the designed anticipation as it does not influence the functioning during floods and can empty excessive water within about 1 day to leave space for consecutive events.

3.2 Selection of blueprinted RLs and design for numerical experiments

To investigate potential joint benefits from RL networks and the sensitivity of their effectiveness to their geographic configurations, several groups of potential RLs upstream are blueprinted (also marked in Fig. 1). Considerations for potential and suitable RL sites are based on terrain slopes, susceptibility to flood, land use conditions, and RL size (area) (Rezazadeh Helmi et al., 2019); specific criteria include: (i) there is free space for constructions (>2500 m^2);

(ii) the slope for the free space is generally mild (iii) serious inundation is observed in the calibration /validation cases. Various types of RL geographic combinations are blueprinted, including (i) series or parallel connections, (ii) aggregated (centralized, with a volume of 40000 m^3) or distributed (decentralized, each with a volume of 13333 m^3) RLs, and (iii) upstream or downstream control. For each blueprinted case, the DEM is then modified by replacing the corresponding elevation with a lower value (usually 4-6 m) to produce simplified RLs; culverts are added to connect the RLs with the Shenzhen River following major roads or straight paths. The blueprinted combinations together with designed cases for numerical experiments are listed in Table 2; corresponding locations of potential RLs can be found in Fig. 1. The design of specific rainfall processes is illustrated in the following subsections.

Table 2 Designed rainstorm scenarios with blueprinted RL configurations for numerical experiments

Cases	Configurations	Rainfall duration (hr)	Return period (yr)	Description
Case 1	No RL	1,2,4,6,9,15	1,2,5,10,25,50,100	before the project
Case 2	RL1	1,2,4,6,9,16	1,2,5,10,25,50,100	current configuration
Case 3	RL1 + RL9 + RL10	4	1,2,5,10,25,50,100	series, upstream control
Case 4	RL1 + RL2 + RL5	4	1,2,5,10,25,50,100	parallel, aggregated, downstream control
Case 5	RL1 + RL2&3&4 + RL5&6&7	4	10,50	parallel, distributed
Case 6	RL1 + RL4 + RL6	4	10,50	parallel, aggregated, upstream control
Case 7	RL1 + RL8 + RL9	4	10,50	series, downstream control

3.3 Frequency analysis and design for extreme rainstorm events

Frequency analysis is carried out for the design of extreme rainfall events in the studied basin based on hourly rainfall records at Ta Ku Ling station in Hong Kong. Peak-Over-Threshold (POT) method is applied for sample selection, because it can take sufficient use of historical events as it selects all events above a certain threshold rather than merely picking up annual maximum and neglecting others (Hosseinzadehtalaei et al., 2020), resulting in a higher value for extreme events compared to the annual maxima-based method. To perform POT, the moving-average technique is first applied to the original time series in order to perform the analysis for various event durations (Willems, 2000). Rainfall events are identified based on the criteria that at least 5-mm rainfall is observed; the rainfall occurring within a 12-hour consecutive period is considered as the same event to guarantee the independence (Willems, 2000). Next, only the events larger than 95 percentiles in terms of maximum hourly rainfall (MHR) and at least the same number of the years are guaranteed are utilized for the calibration of probability distribution models. For a reference, based on hourly rainfall data, a total of 1409

events with mean MHR of 15.3 mm and mean duration of 4.4 hours are identified. Finally, there remain 72 events with MHR > 35 mm, larger than the Yellow Rain Warning in Hong Kong (30 mm/hr).

To estimate the event size corresponding to different exceeding frequencies, a variety of probability distribution models that are widely used in hydrological extreme event analysis are tested, including generalized extreme value (GEV) distribution, generalized Pareto (GP) distribution, Log Pearson Type-III (Gamma) (LP3) distribution, and Weibull (WB) distribution (Johnson, 1995), respectively. The best parameter estimation is selected among all the groups of parameters, based on the coefficient of determination between sample data and the predicted values from the model. In addition, the Anderson-Darling test as well as Chi-square test (Meylan, 2019) are conducted for the calibrated distribution models; the RSME of the probability between calibrated models and sample points are also calculated for reference. The results of frequency analysis are plotted in Fig. 3 including identified events of various durations and best-fit LP3 curves. The performance of the 4 probability models based on the 4 criteria are ranked to 1 to 4 (the higher the better) and presented in the subplot of corresponding durations. Although all the models perform reasonably well, the LP3 distribution generally performs the best, and then is the Weibull distribution, while the GP distribution has the worst overall performance.

A global design of idealized rainstorm events is then performed covering different event sizes (intensity and duration). For each exceeding probability (or return period, which is discretely selected at 1-year, 2-year, 5-year, 10-year, 25-year, 50-year and 100-year), predicted rainfall intensity is plotted against duration and fitted into the following empirical relationship to obtain Intensity-Duration-Frequency (IDF) curves (and plotted in Fig. 3b).The Chicago hyetograph is adopted for the design of rainfall process so that for each duration the rainfall intensity is congruent with the IDF curve, yielding a conservative estimation (Alfieri et al., 2008). The continuous rainfall process is then discretized into 5-min bins when applied as the boundary condition in the rainfall-runoff simulation. 3 example events are presented in Fig. 3c. The design of simulation cases is summarized in Table 2.

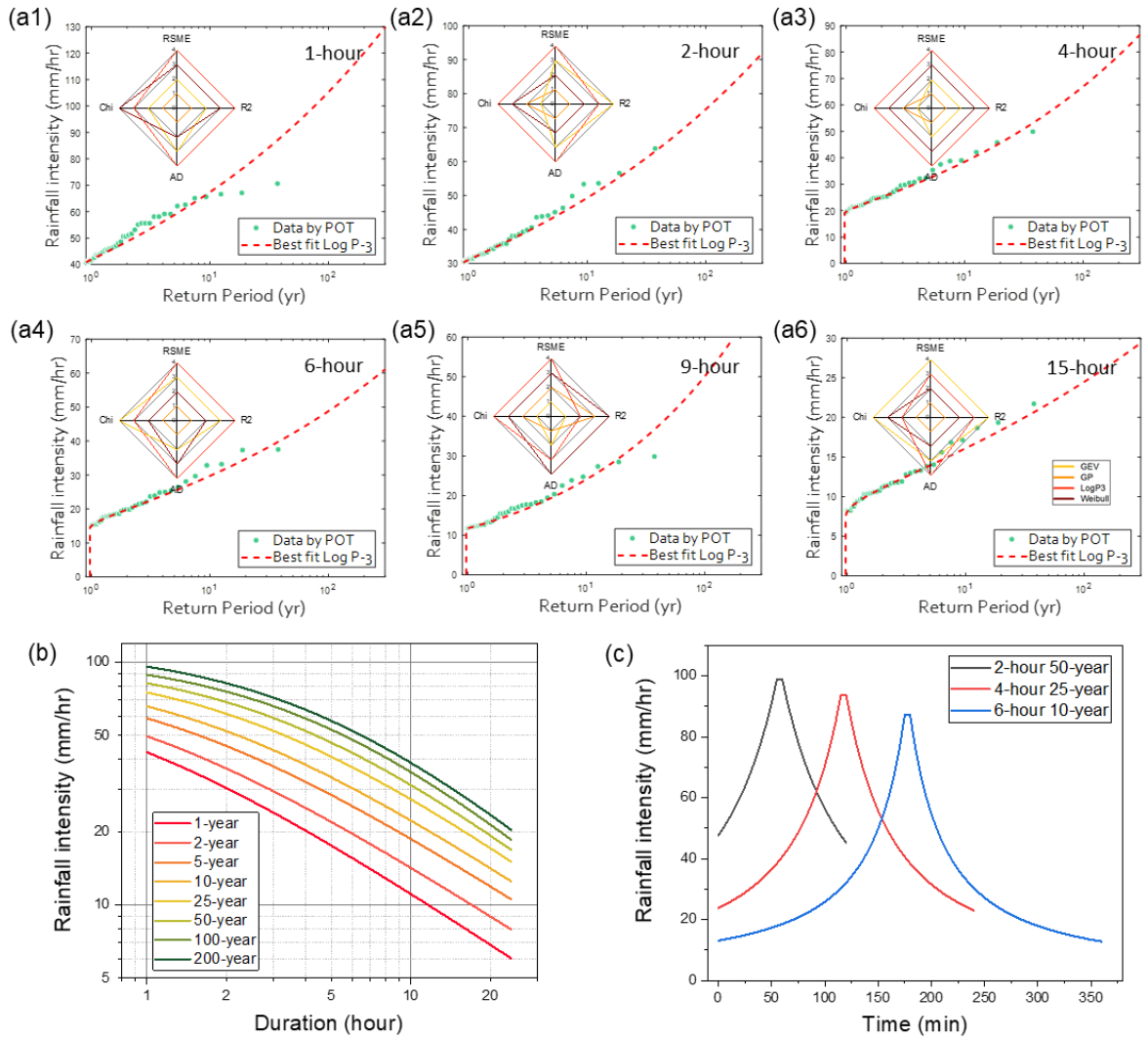

Fig. 3 Frequency analysis and design of rainstorms. (a1)-(a6) show identified and fitted Log-P3distributions of events with various durations; the subplots of radar maps show the performance of 4 probability models based on the 4 criteria namely Chi-Square test (Chi), Anderson-Darling test (AD), coefficient of determination (R2) and RSME; (b) shows the IDF curve constructed based on the frequency analysis; (c) plots 3 examples of designed rainstorm based on Chicago model.

3.4 Criteria for effectiveness assessment of RLs

To evaluate the performance of different river-RL systems in response to various rainfall events, simulation results are analyzed from both local and entire-catchment perspectives. From localized perspective, we evaluate the rate of reduction of peak runoff in the hydrograph (relative to the current system or the system without any RLs, whichever is noted), the delay of peak time (positive value means retarded peak), the change of peak duration as well as accumulated peak volume (the peak is defined as the part in the hydrograph higher than 75% of the peak value). From the entire-catchment perspective, the maximum inundation is processed to be a uniform-sized raster, and the spatial difference of the maximum inundation between a blueprinted case with the current system is also calculated.

4 Results

4.1 Model calibration and validation

Model calibration is first carried out based on the consecutive event occurred on August 28-30, 2018, containing the maximum runoff (80 m^3/s) measured within 2018-2020 and the maximum rainfall event was comparable to a 10-year event. The calibration is targeted at Manning's coefficients for different land use types although they are preset according to the reference manual (Brunner, 2021); final model parameters are listed in Table 3. The calibrated result shows reasonable accuracy (Fig. 4); discrepancies are ascribed to rainfall spatiotemporal variability, DEM accuracy, neglect of small drainage and the model itself. The discrepancy for the small runoff at the early stage (Fig. 4a) is also likely due to the neglect of the contribution of antecedent event. Another 10 events within the time span of data availability are also identified for model validation. Both the simulated values of flood duration as well as peak runoff agree with the measurements (Fig. 4b&c). The overall performance of the model indicates a reliable performance for further application under current data availability.

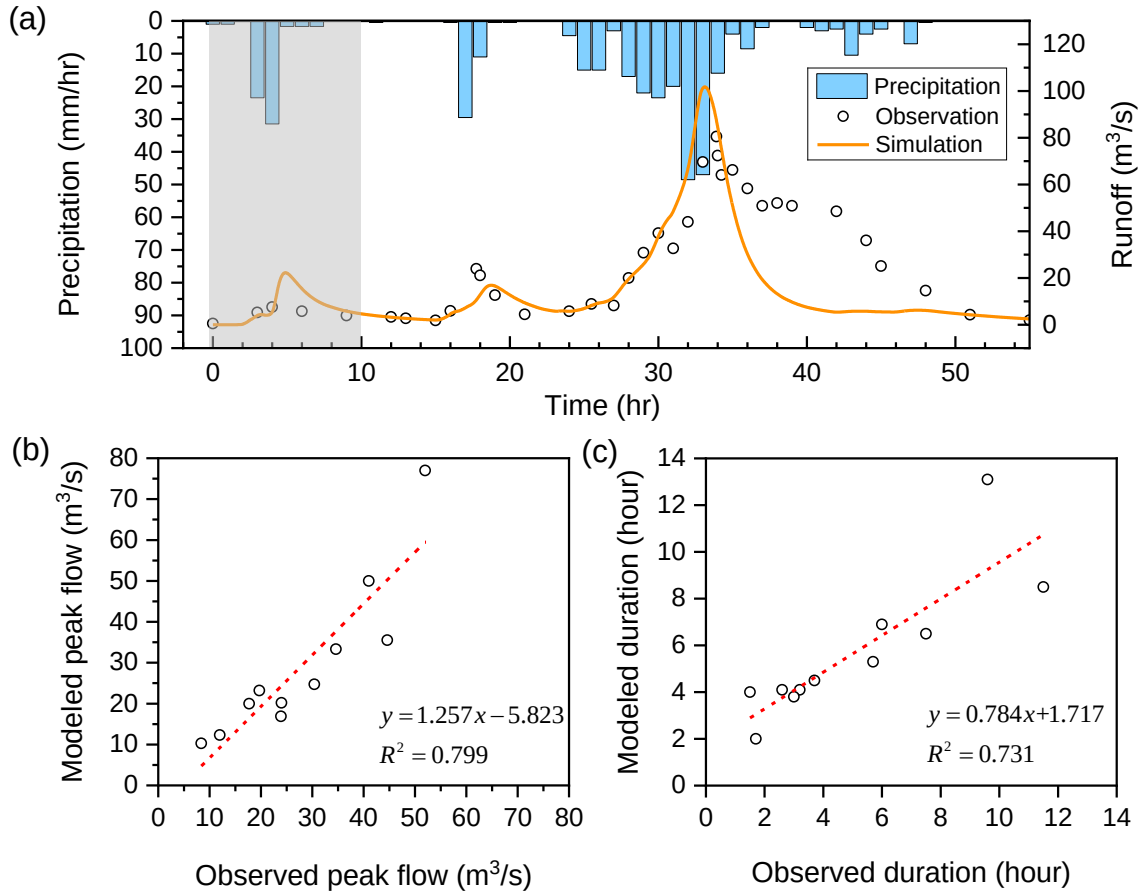

Fig. 4 Model calibration (a) and validation of flood peak (b) and duration (c) based on measured events during 2018-2020.

306 **Table 3** Calibrated parameters for hydrodynamic modeling

Landcover Classification	Mannings Coef. ($sm^{-1/3}$)	Percent Imperviousness (%)
grassland	0.06	20
open water	0.03	100
bareland	0.025	30
building area	0.2	75
forest	0.2	0

307

308 ***4.2 Hydrological response of the existing river-RL system***

309 *4.2.1 Typical hydrologic response*

310 The existence of the current RL modifies the pattern of hydrological response especially for
311 events with a certain range of magnitude and duration. For the events with maximum water
312 surface elevation (WSE) not higher than the wire (8.4 m), corresponding to a return period
313 smaller than 10 years for the 2-hour event, for example, the RL can hardly make any effect. For
314 larger events, the influence of the RL can generally be classified into 4 stages, as shown by the 4
315 typical stages in Fig. 5.

316 • **Stage-I**: The RL reduces the peak runoff, but the peak time of the two cases is almost the
317 same (Fig. 5a, 25-year event with 2-hour duration). Only a small volume of water enters the
318 RL and the maximum WSE (at t1) is lower than the wire elevation (8.4 m). This is
319 understandable because the flow through the wire increases monotonously with the WSE in
320 the channel (thus on top of the wire) so that the wire flow has no phase difference with the
321 outside flood wave. The RL WSE gradually decreases as water releases to the channel
322 through the culverts (first through both culverts and then only through the downstream one)
323 until no WSE difference exists for both sides.
324 • **Stage-II**: The RL obviously reduces the peak runoff and delays the peak time, which is the
325 most ideal outcome that fulfills the design purpose (Fig. 5b, 50-year event with 2-hour
326 duration). The maximum WSE just exceeds the wire elevation, inducing a small amount of
327 negative flowrate, which indicates a reversing flow from the RL back to the channel, leading
328 to the second rise of the outside hydrograph. But because the reversing flow is very small
329 compared to the external flood, the slope of the rising limb is almost the same with Case 1.
330 The WSE in RL rapidly falls below the wire elevation, and then gradually decreases like
331 Stage-I.
332 • **Stage-III**: Shown in Fig. 5c (50-year event with 4-hour duration), the RL only has a small
333 but detectable effect for both peak time delay and peak reduction, the slope of the rising limb
334 of the hydrograph of Case 2 can be steeper than Case 1, due to the much larger reversing
335 flow from the RL compared to the second stage. The period of reversing flow becomes
336 much longer than Stage-II (from t2 to t3) while the maximum flowrate (about 5 m^3/s) does
337 not see obvious change, since the WSE inside and outside of RL roughly declines with the
338 same speed.
339 • **Stage-IV**: It reaches the fourth stage if the event size further increases as shown in Fig. 5d

(100-year event with 9-hour duration), the RL almost has no pragmatic effect, as the capacity is running out even before the flood reaches peak period. There is a longer duration of positive wire flow and higher RL WSE due to the long-lasting rising limb of the outside hydrograph, while the time of maximum reversing flow is brought forward because the falling WSE for the outside channel occurs much more slowly compared to the RL.

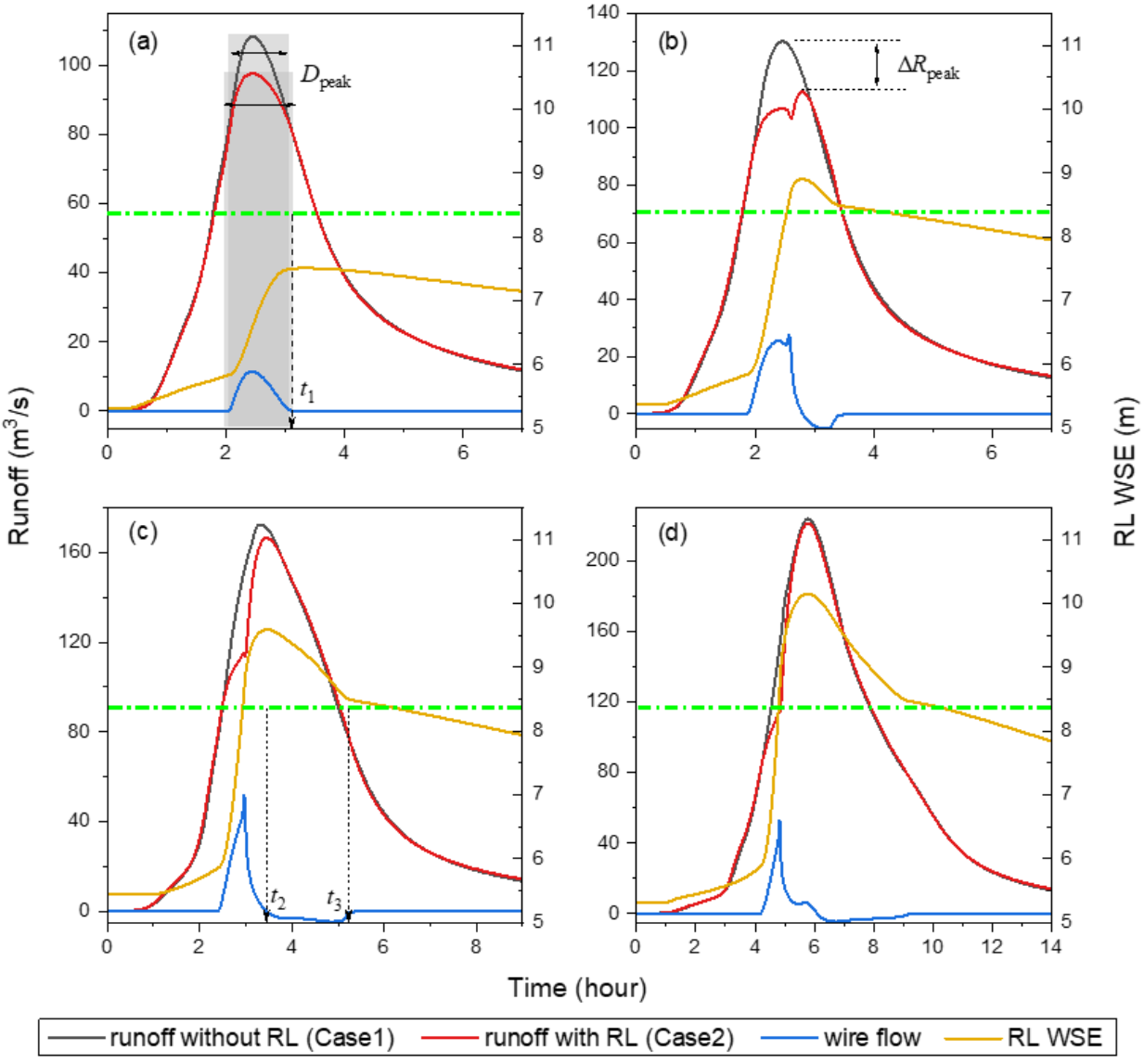

Fig. 5 Typical stages of RL function as a result of river-lake interaction with an example for each stage, viewed at the near downstream location of the RL (S4). (a) Stage-I, 25-year event with 2-hour duration; (b) Stage-II, 50-year event with 2-hour duration; (c) Stage-III, 50-year event with 4-hour duration; (d) Stage-IV, 100-year event with 9-hour duration. The green dashed line marks the wire elevation (8.4 m); the grey shadow marks the peak flood period.

4.2.2 How RL affects pre-constructed streamflow under varying events

353 The effectiveness of the current RL in the global design of events is assessed through 4
354 perspectives , including the rate of reduction of peak runoff compared with Case 1, change of
355 peak volume, arrival time and duration (Fig. 6). It is seen that the RL reduce the peak runoff,
356 reduce peak volume and duration, retard peak arrival time up to about 14%, 25%, 25 min, and 20
357 min, respectively. The RL generally has a decent performance within an L-shaped band limited
358 by event duration and exceeding probability. The L-bands generally lie at moderate return
359 periods (10- to 25- year) combined with large durations (> 6 hours) towards small durations (< 4
360 hours) combined with large return periods (> 25-year). In spite of the similarities, different
361 characteristics of the effectiveness pattern can be drawn from the 4 criterions: (1) *the L-band for*
362 *peak reduction* (Fig. 6a) is located most towards small return periods, indicating the peak
363 reduction effect favors small or moderate amplitude events, and the RL can make such effect as
364 long as the event causes water level higher than the wire elevation; (2) *the L-bands for peak*
365 *volume and peak duration* (Fig. 6b & d) are much wider without rebounding back to nullity with
366 the increase of return periods, due to the sufficient interaction between the river and the RL; (3)
367 *the L-band for peak time* (Fig. 6c) is almost perpendicular to the return period axis for large
368 durations, meaning that the time delay effect is insensitive to the variation of event duration if it
369 lasts long (more than 6 hours), probably because the time to fill up the RL does not change
370 considerably further with the increasing event duration; (4) *the L-band for peak reduction* (Fig.
371 6a) tends to be insensitive to the return period for small-duration events (< 4-year), as the
372 maximum capacity is not reached yet (e.g. for 2-hour 100-year event the maximum volume in
373 the RL only reaches 78% of the capacity, while for 1-hour 100-year event the maximum WSE in
374 the channel is even slightly below (5 cm) the wire elevation), indicating that the RL has much
375 more potential to deal with more extreme events (> 100-year) with a short duration (< 2-hour).
376 Moreover, owing to different focuses of the 4 criteria, the combinations of return periods and
377 event durations for the optical performance does not coincide. For example, within the coverage
378 of the current simulation, 2-hour 50-year event has the largest peak reduction (14%), while 6-
379 hour 25-year event has the largest peak duration reduction (20 min). In this regard, various
380 criteria are suggested to be taken into account for a comprehensive judgment or decision making.

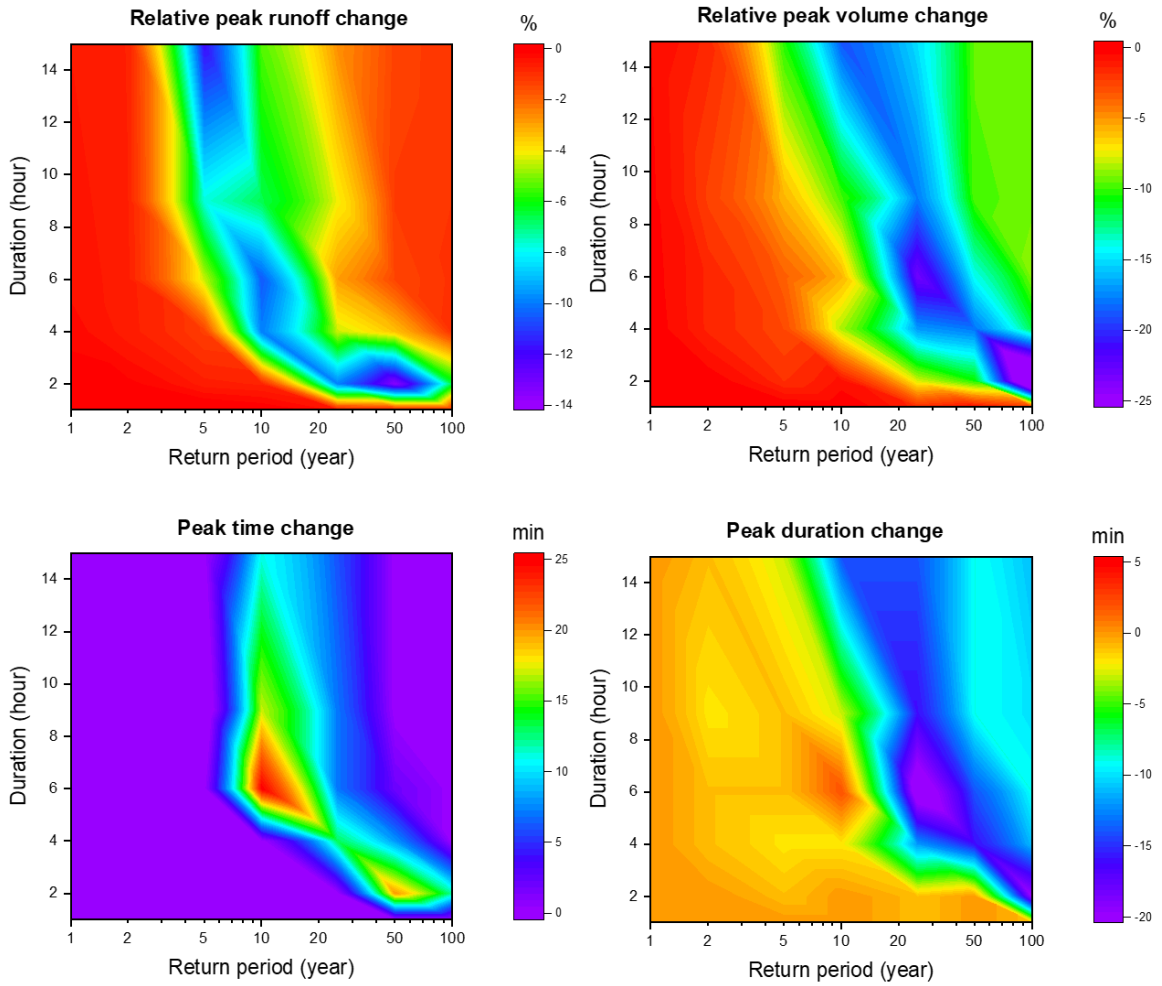

Fig. 6 Effectiveness of the RL viewed from four criteria under global rainfall scenarios.

4.3 Hydrological and hydraulic effects of blueprinted RLs

4.3.1 Series V.S. parallel connections

The performance of RLs in series (Case 3) and parallel (Case 4) connections with aggregated capacity (40000 m^3 for each RL) under different return periods are analyzed in this subsection. Fig. 7 plots the comparison of the peak runoff between Case 2 and Case 3 or 4 at 3 different locations (Fig. 1). First, additional RLs can provide positive effects in the reduction of peak runoff. Along the main channel (S1 and S4), the performance of Case 3 is generally better than Case 4, although the difference is not apparent for moderate-to-large events while series connection leads to considerably small peak runoff for 1-year to 2-year events. This is because, for small events, the RLs connected in series with the Shenzhen River have sufficient time to interact with the river channel and release the peak flow, while the RLs in parallel connection only interact partially with flow paths and cannot be fully involved; for extreme events (> 50-year) that far beyond the capacity of an individual RL, the downstream peak runoff is dominated by the increasing and speeding excessive water accumulation rather than the cut-off by the RL fa

upstream. However, for the location S3, the parallel connection (Case 4) can reduce 3-5 m^3/s of the peak runoff while the series connection (Case 3) has the same outcome as Case 2, because the new RLs located in the main channel can hardly influence the tributary watersheds. In addition, it is noteworthy that the amount of peak runoff reduction at S4 is the least for the 10-year event (both for Case 3 and Case 4) although the best performance in the 4-hour event is achieved for the downstream RL in Case 2 (Fig. 7a). As the upstream RLs alter the duration and amplitude of the flood entering S3, the amount of water fed into the downstream RL is changed correspondingly, which is 34000 m^3 for Case 2 and about 20000 m^3 for Case 3 and Case 4. In other words, additional modifications of the current lake-river system can alter the pattern of overall hydrological response, thus a catchment-scale analysis rather than separate consideration of individual RLs is essential for the optical design of joint NBSs.

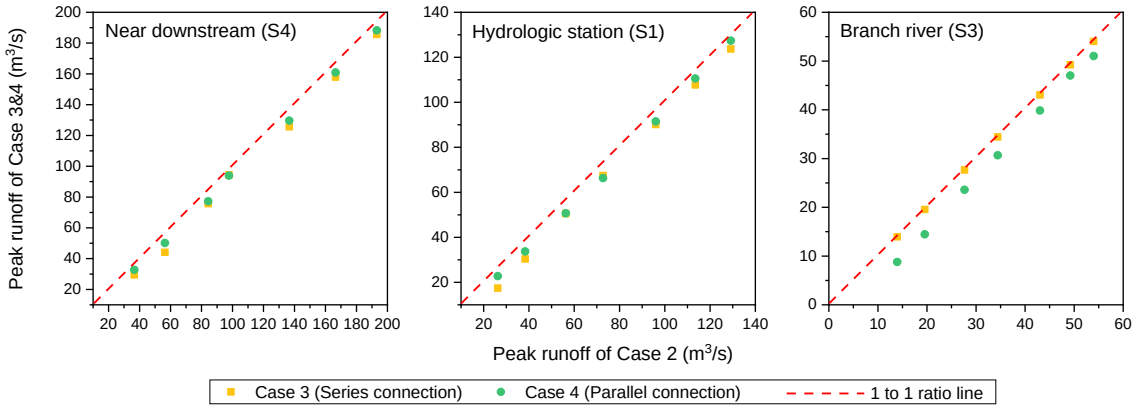

Fig. 7 Comparison of peak runoff at 3 different locations between Case 3&4 and Case 2. Note: the 7 scatter points in each subfigure represent the quantity from 1-year to 100-year events as the magnitude increases

Spatial patterns of maximum inundation mitigation (compared with Case 2) are plotted in Fig. 8 b1, b2, c1 & c2. It is clear that the series connection only provides benefits for the main channel while the parallel connection can extend the influence on a wider range away from the river channel. It is also shown that the RLs almost have no benefits to their upstream region; it can even be observed that a slightly larger maximum water depth exists around the RLs probably due to the backwater effect. The 50-year event cases provide similar spatial patterns with the 10-year events except that the reduced maximum inundation depth is smaller.

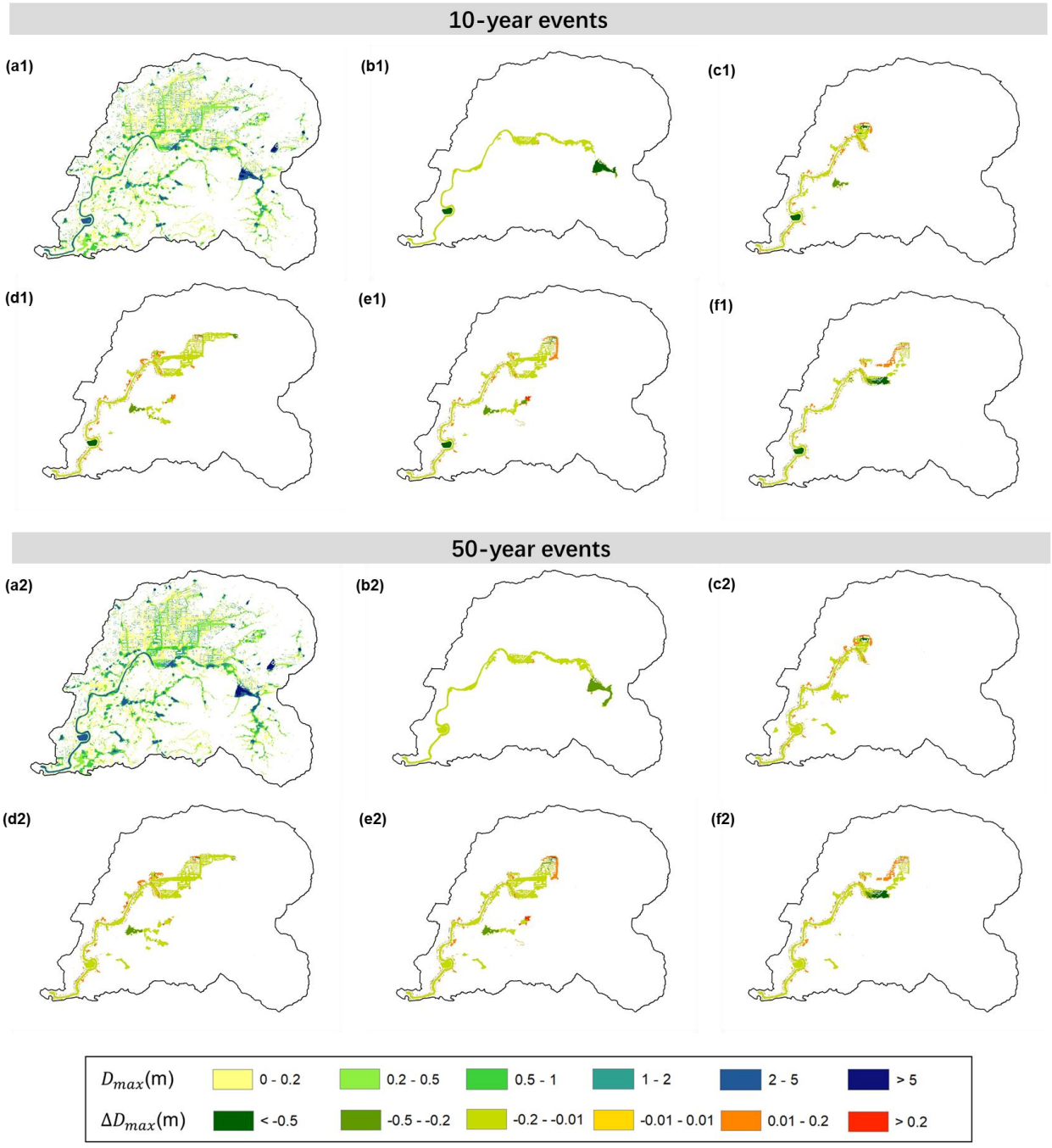

Fig. 8 Spatial distribution of maximum inundation D_{max} (Case 2, for a1 and a2) and the change of maximum inundation ΔD_{max} (Cases 3-7) of 10-year (subscript 1) and 50-year events (subscript 2). Sub-figures b-f represent the results of Case 3 to Case 7 subtracted by the results of Case 2.

4.3.2 Aggregated V.S. distributed RLs

For blueprinted RLs in parallel connection, we have compared the effectiveness of aggregated (Case 6) and distributed (Case 5) placement in terms of peak runoff reduction, based on 4-hour events with 10-year and 50-year return periods. Fig. 9 shows the rate of peak reduction

at near downstream of the current RL (S4), the hydrologic station (S1), and the mouth of the tributary (S3). The tributary watershed has a great potential to be benefited from additional RLs, with the rate of peak reduction of more than 10% for 10-year event and 7% for 50-year event, respectively. The aggregated setting is more effective than the distributed one, as the selected RL site is in series connection with the tributary channel. For the other two locations along the mainstream of the Shenzhen River, the distributed setting performs better in all the cases, with a rate of peak runoff reduction ranging from 3% to 5.3%. The spatial pattern of maximum inundation (Fig. 8) shows that the both settings lead to roughly the same magnitude of inundation depth reduction compared to Case 2, but a relatively larger area can benefit from the distributed setting of Case 5, in which the area that suffers from backwater-induced aggravated inundation is also smaller compared to the aggregated setting of Case 6.

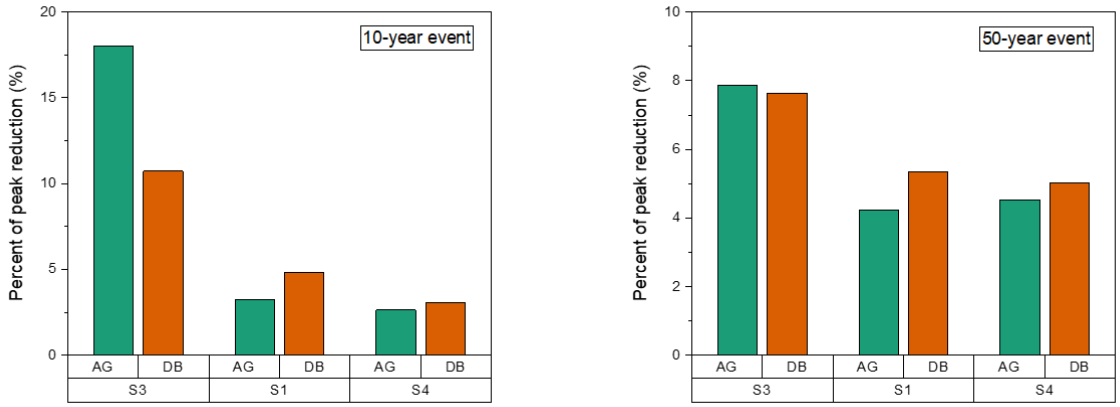

Fig. 9 Summary of system performances (rate of peak reduction) of aggregated (AG) and distributed (DB) configurations at 3 different locations: the outlet of the tributary beside the RL (S3), hydrologic station (S1) and near downstream of the RL (S4).

4.3.3 Upstream control V.S. Downstream control

In addition to the degree of centralization as well as parallel/series connection, the effectiveness of being upstream and downstream control is analyzed by comparing Case 7 (downstream control in series) with Case 3 (upstream control in series) and Case 4 (downstream control in parallel) with Case 6 (upstream control in parallel). The rate of runoff peak reduction at the near downstream point of the current RL (S4) is summarized in Fig. 10. While the series connection cases consistently provide slightly better results for channel downstream in both 10-year and 50-year events, it is interesting to observe that whether upstream or downstream control is more effective highly depends on event magnitude. Further inspection of the rate of usage of individual RLs in different cases indicate that the downstream control cases have already run out of the total capacity of each RL in the 10-year event (e.g., 100% for both RLs in Case 4 while 89% and 50% for the RLs in Case 6) and thus has no extra space for further peak reduction in 50-year event, unlike upstream control cases (e.g., the usage of RLs in Case 6 further increases to 95% and 80%). Therefore, the RLs system could potentially achieve better performance if the RL with greater capacity is placed closer to downstream, as also discussed in Ayalew et al. (2015). Despite the inferiority according to the locally based results, the downstream controlled series connection settings (Case 7) can provide a greater area of inundation mitigation along the

channel compared to upstream control (Case 3) for both 10-year and 50-year cases as shown in Fig. 8, but the benefit hardly extends upstream. However, the downstream controlled parallel settings (Case 4) do not share the same advantage over the upstream control settings (Case 6), due to the early exhaust of capacity. The results above suggest that the effective drainage area upstream of the RLs relative to individual capacities, as well as the threshold that RL-river interaction occurs, are both essential parameters that control the individual and overall effectiveness regardless of types of configurations, as such, there is unlikely to be a universal answer for an optical recommendation unless the event conditions, terrain features as well as RL settings are jointly considered.

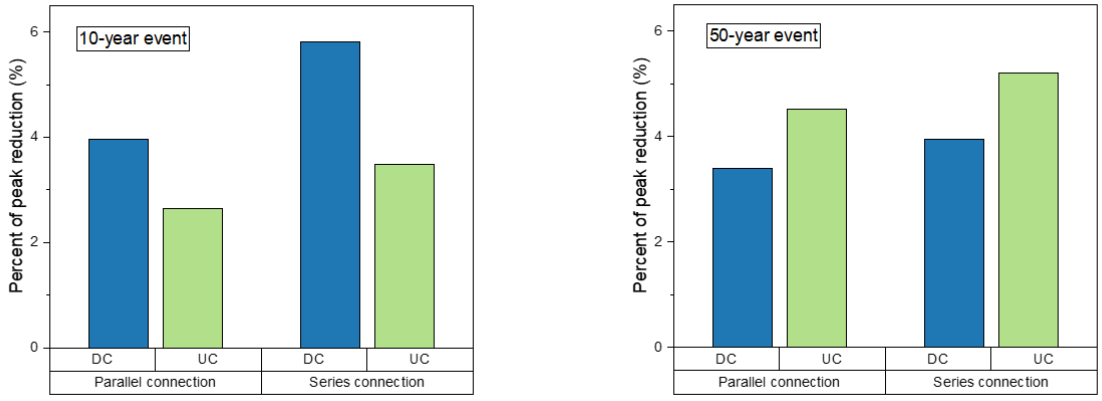

Fig. 10 Summary of system performances (rate of peak reduction) upstream and downstream control (DC and UC respectively) configurations at 3 different locations.

5 Discussions

5.1 Effects of spatial and temporal rainfall variability

The primary numerical experiments assume a uniform rain field across the entire basin and a single rainfall temporal pattern of the Chicago hyetograph for each event. However, rainfall events may occur with spatially varying intensities at the same time, or with complex hyetographs (including consecutive events) over sometime, or both. As widely discussed in previous studies, the above situations are nontrivial at all in terms of catchment hydrological response across different land cover features (Cristiano et al., 2017; Zhu et al., 2018), failure to consider the spatiotemporal variability with a resolution higher than a certain threshold (also controlled by catchment scales) results in the greater uncertainties and inaccuracy (Cristiano et al., 2019; Ochoa-Rodriguez et al., 2015). Studies based on natural catchments suggest 5 min (or below) and ~1 km rainfall inputs are required to sufficiently capture the effect of rainfall variability for a drainage area of ~ 1 - 100 ha, while the applicability has not been corroborated for urban catchments using hydrodynamic models (Ochoa-Rodriguez et al., 2015). For the studied catchment, 5 additional simulation cases are designed to preliminarily inspect the influence of rainfall structures: (i) for temporal variability, consecutive events (10-year + 50-year with 4-hour duration and its reverse) with 5-hour intermittency are simulated; for spatial variability, single events with 10-year intensity in Hong Kong and 50-year intensity in Shenzhen with 4-hour duration and its reverse are simulated. The results in Fig. 11 indicate that for the influence of temporal variability (Fig. 11 a1&b1), the hydrographs of the first sub-events are

identical regardless of event size, while the second sub-events lead to considerable higher peaks compared to the corresponding return periods. To be more specific, the second 10-year event has a peak 50% larger than the single event and the peak of the second 50-year event is also 22% larger than the single one. As the total volume accumulation for the two groups of consecutive events (and the single events within their periods) are identical (Fig. 11 b1), it is inferred that the surface storage of the former events significantly alters the routing of the latter one by reducing their potential surface inundation as well as transit time, due to the occupied surface inundation capacity and shortened flow-paths. The increased hydrographs and partially filled RL cause the performance of the RL-river system of the consecutive 10-year event to be similar to the 25-year single event, while that of the 50-year event to approach to the 100-year single event. In comparison with temporal variability, the influence of rainfall spatial non-uniformity (Fig. 11 a2&b2) is much smaller, which is consistent with previous findings (Yang et al., 2016; Zhu et al., 2018). The case with 50-year event at the Shenzhen side and 10-year event at the Hong Kong side turned out to be more dangerous than the reversed case and the uniform case (25-year event for the entire catchment). Viewing from total volume accumulation (Fig. 11 b2), the case with the 50-year event at Hong Kong side exhibits a smaller volume compared to the other two cases, which manifests a larger capability of water storage in the rural region of Hong Kong side. In contrast, there is less blocking effect in the urban region at Shenzhen side as a greater amount of water is drained to the river channel ultimately. The results above indicate consecutive events and uneven spatial rainfall configurations may potentially bring more serious burdens for RLs and thus higher flood risk, compared to the single events with a regular hyetograph and spatially uniform rain fields in conventional designs.

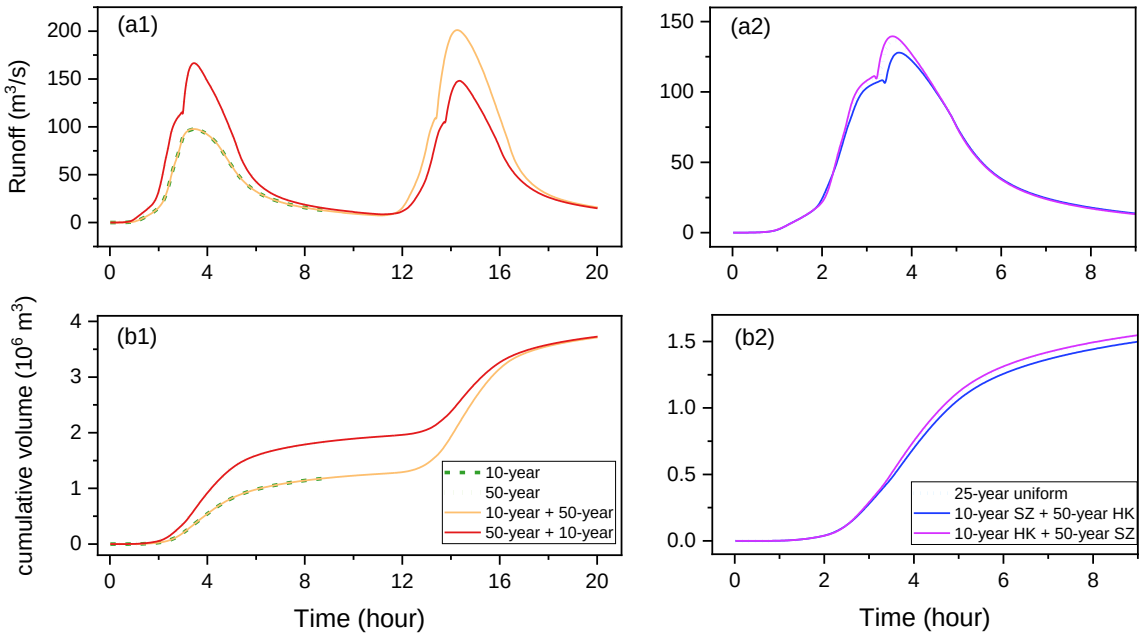

Fig. 11 Influence of spatiotemporal rainstorm variability on the hydrologic response of the RL-catchment system at S4. (a1) the hydrograph of 10-year, 50-year, sequent of 10-year and 50-year, and sequent of 50-year and 10-year events; (a2) the hydrograph of 25-year event with spatially uniform rain field, 10-year event in Hong Kong and 50-year event in Shenzhen, and 50-year event in Hong Kong and 10-year event in Shenzhen; (b1) the runoff volume accumulation of (a1); (b2) the runoff volume accumulation of (a2).

5.2 Potential improvement of the RL-river system

The performance of the RL-river system in response to extreme flood events can be potentially improved by modulating the interactions between individual RLs and the entire basin. As indicated in the results (Section 4.1), optimal performance of an RL is limited to a range of rainstorm intensity and duration under a static setting. Specifically, four stages of the RL function can be characterized with the increase of event size (both duration and intensity), in which the second stage is most favored. The crux is the design of the wire (shape, elevation, dimensions, materials, etc.) connecting the river channel and RLs, which directly determines the demarcation between Stage-II and Stages- I & III A simple scatter (Fig. 12) can help to illustrate the RL performance (based on peak runoff reduction) demarcated into 4 stages (although not quantitatively). With the increase of event size (both duration and intensity), the accumulated inward flow increases (noted as retention volume and normalized by the designed capacity), the rate of peak reduction first increases monotonously (albeit at a small level, in Stage-I) and soon reaches a relatively high level, when the retention volume is about 30%-70%. The reversed flow is not remarkable until Stage-III, when the effectiveness rapidly decreases at the same pace with the increase of normalized reversed flow. In Stage-IV, the RL fails to provide effective retention; the reversed flow slightly decreases as new connections between the RL and the channel emerge due to flow overbanking. In order to extend the range of Stage-II to the most degree under limited designed capacity, one may consider limiting the potential maximum reversed flow by reducing the elevation difference between the wire and the bank and reducing the slope of the reversed flow curve by preventing outward flow by extra control devices. By this way, the range of Stages- III & IV will be pressed. For depressing the range of Stage-I (the RL functions for smaller events) while keeping the current effectiveness for larger events, additional culverts with controllable gates at lower elevations (than the wire) connecting the upstream channel with the RL may be considered. As for the blueprinted RL network, both local hydraulics of RLs and global hydrology of the catchment should be scrutinized to improve their performance due to the space-time disparity of RLs' functions and event-dependent routing characteristics. For example, in the distributed parallel connection case (Case 5), upstream RLs are placed in face to water accumulation earlier than downstream ones while the durations are relatively smaller (same with other cases of blueprinted network); the rate of water accumulation in RLs of Hong Kong side tends to be longer compared to Shenzhen side for the 10-year event (the time used to reach the maximum depth is about 70 min, 70 min and 180 min in Hong Kong while 50 min, 60 min and 150 min in Shenzhen), while no significant difference can be discerned for the 50-year event. Additional complexity exists in reality, as the RL system may work jointly with grey infrastructures, such that future efforts for both surrogate models of RL-catchment systems as well as optimization techniques are indispensable. In addition to the static designs or passive systems, dynamic controls of the stormwater infrastructure network can potentially provide remarkably better overall performance especially for large events (30-year or more). Moreover, it can offer viable solutions to adapt to individual event conditions in a real-time manner (Wong & Kerkez, 2018).

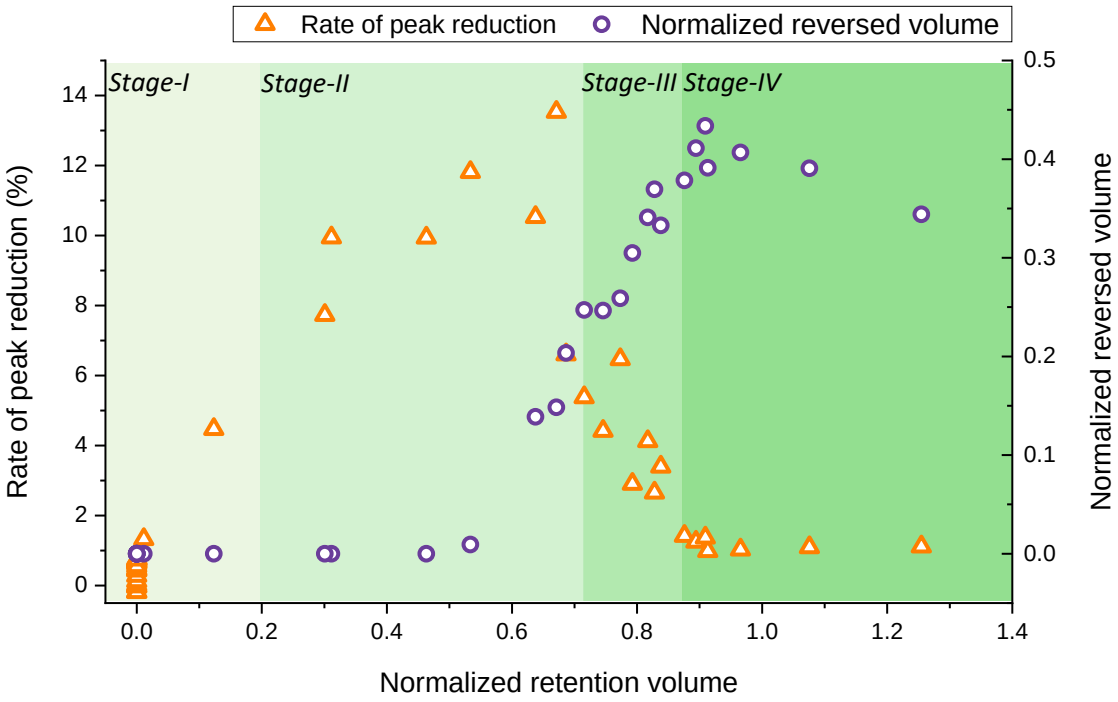

Fig. 12 The relationship between RL utility (accumulated inward wire flow normalized by the capacity) and the rate of flood peak reduction at near downstream location (S4), and the relationship between RL utility and accumulated reversed volume normalized by the capacity. 4 stages of RL function are qualitatively demarcated based on the rate of peak reduction.

5.3 The limitations of the current study

We are aware of the following major limitations along with this study. First, the urban drainage network, particularly in the urban region of the Shenzhen side is not considered in the model. Plenty of studies demonstrates that the use of drainage systems causes increases in runoff volume, peak flowrate and reduction in runoff duration and time to the peak although the degrees vary with system properties (Guan et al., 2015a; J. D. Miller et al., 2014; Rogger et al., 2017). However, it is also true that overall good agreement can be achieved for both flood peak and duration by the calibrated model for the measured storm events, suggesting that the impact of existing drainage systems on the hydrologic response of the entire catchment is limited. Nevertheless, neglect of subsurface drainage leads to overestimation of surface inundation and may obscure the locations with actually high risks, as such, to more faithfully model urban flood inundation processes, it is recommended to be considered in future studies. Second, the hydrodynamic model relies heavily on high-quality DEMs, low resolution or erroneous representation of surface elevation may cause disconnection of flow paths and significantly alter surface hydrologic patterns, which is also the common challenges faced by other studies using hydrodynamic models (Horritt & Bates, 2001; Jarihani et al., 2015; Saksena & Merwade, 2015). Third, carrying out systematic numerical experiments by the catchment-scale hydrodynamic model under globally designed scenarios is still very computation-intensive compared to hydrologic models, for example, a PC equipped with Intel i7-9700 CPU with 16 GB RAM and 8 cores has a real-time/simulation-time ratio of 0.8 under the numerical settings of this study.

Finally, the study scope at the current stage has not been systematically extended to the impacts of spatiotemporal characteristics of local climatology nor the nonstationary frequency concerning climate change, which brings us strong pulses for future work.

6 Conclusions

To bring insights into how flood retention lakes can better function in a rural-urban catchment, we carry out systematic numerical experiments by a full 2D hydrodynamic model. The model proves its capability in predicting flooding processes with reasonable accuracy, including the dynamic interactions between RLs and the river channel. Comparison of simulation results of cases with and without the current RL indicates that the decent effectiveness in terms of delay of runoff peak time and reduction of peak runoff, peak volume and duration generally lies in an L-shaped band limited by a certain range of rainstorm intensity of duration, where large return periods (> 25-year) combine with small durations (< 4-hour) or moderate return periods (10- to 25- year) combine with moderate to large durations (> 6-hour), whereas the exact optimal combinations under the 4 criteria are different. With the increase of the event size (duration and intensity), 4 typical stages of RL function are identified while the second stage represents the most favored mode as the RL both damps the peak runoff and delays the peak time remarkably, due to effective flow diversion during the peak flood period with negligible reversing flow to the channel. Additional blueprinted RLs further reduce the maximum surface inundation and peak runoff compared to the current layout mainly downstream of the RLs. The series connection shows slightly better capability viewed along the river channel, while the parallel connection can provide benefits to sub-watersheds. The distributed setting has a better overall performance compared to the aggregated setting with the same total capacity, with a larger area of maximum inundation reduction. The downstream control RL configurations tend to perform better for moderate events (10-year) while the upstream ones are superior for extreme events (50-year). Besides, potential impacts of spatiotemporal rainstorm variabilities on the RL-river system are discussed. Consecutive events with the same hyetograph may cause flood peaks much larger than a single event with the same return periods; rainstorms concentrated more at Shenzhen side (with dense urban regions) result in a higher flood peak compared to spatially uniform cases. Discussions also suggest that different composition of retention and reversed RL volume as the result of RL-river interaction may serve as an indicator on their benefits for flood mitigation for the entire catchment.

Acknowledgements

This study is financially supported by Environment and Conservation Fund Project (ref: 108/2019) from Hong Kong Environmental Protection Department, General Research Fund (No. 17202020) from Hong Kong Research Grants Council, and Youth Program of National Natural Science Foundation of China (NO. 51909227). We would like to thank the Shenzhen River Regulation Office of Water Authority of Shenzhen Municipality for providing river cross section data and hydrological data. In addition, we sincerely appreciate Dr. Songbai Wu who provides part of the computing device that fastens the speed of numerical simulation.

Data Availability Statement

The datasets that support this study is available at http://doi.org/10.5281/zenodo.5853044. The software exployed to perform the numerical simulations in this study, Version 6.0 of HEC-RAS, can be downloaded from https://www.hec.usace.army.mil/software/hec-ras/download.aspx.

References

Alfieri, L., Laio, F., & Claps, P. (2008). A simulation experiment for optimal design hyetograph selection. Hydrological Processes, 22(6), 813–820. https://doi.org/10.1002/hyp.6646

Ayalew, T. B., Krajewski, W. F., & Mantilla, R. (2015). Insights into Expected Changes in Regulated Flood Frequencies due to the Spatial Configuration of Flood Retention Ponds. Journal of Hydrologic Engineering, 20(10), 04015010. https://doi.org/10.1061/(ASCE)HE.1943-5584.0001173

Bates, P. D., Horritt, M. S., & Fewtrell, T. J. (2010). A simple inertial formulation of the shallow water equations for efficient two-dimensional flood inundation modelling. Journal of Hydrology, 387(1–2), 33–45. https://doi.org/10.1016/j.jhydrol.2010.03.027

Bellu, A., Sanches Fernandes, L. F., Cortes, R. M. V., & Pacheco, F. A. L. (2016). A framework model for the dimensioning and allocation of a detention basin system: The case of a flood-prone mountainous watershed. Journal of Hydrology, 533, 567–580. https://doi.org/10.1016/j.jhydrol.2015.12.043

Birkinshaw, S. J., Kilsby, C., O'Donnell, G., Quinn, P., Adams, R., & Wilkinson, M. E. (2021). Stormwater Detention Ponds in Urban Catchments—Analysis and Validation of Performance of Ponds in the Ouseburn Catchment, Newcastle upon Tyne, UK. Water, 13(18), 2521. https://doi.org/10.3390/w13182521

Brunner, G. W. (2021). HEC-RAS, River Analysis System Hydraulic Reference Manual. 546.

Chen, C.-N., Tsai, C.-H., & Tsai, C.-T. (2007). Reduction of discharge hydrograph and flood stage resulted from upstream detention ponds. Hydrological Processes, 21(25), 3492–3506. https://doi.org/10.1002/hyp.6546

Cohen-Shacham, E., Walters, G., Janzen, C., & Maginnis, S. (Eds.). (2016). Nature-based solutions to address global societal challenges. IUCN International Union for Conservation of Nature. https://doi.org/10.2305/IUCN.CH.2016.13.en

Cristiano, E., ten Veldhuis, M.-C., & van de Giesen, N. (2017). Spatial and temporal variability of rainfall and their effects on hydrological response in urban areas – a review. Hydrology and Earth System Sciences, 21(7), 3859–3878. https://doi.org/10.5194/hess-21-3859-2017

Cristiano, E., Veldhuis, M., Wright, D. B., Smith, J. A., & Giesen, N. (2019). The Influence of Rainfall and Catchment Critical Scales on Urban Hydrological Response Sensitivity. Water Resources Research, 55(4), 3375–3390. https://doi.org/10.1029/2018WR024143

David, A., & Schmalz, B. (2020). Flood hazard analysis in small catchments: Comparison of hydrological and hydrodynamic approaches by the use of direct rainfall. Journal of Flood Risk Management, 13(4). https://doi.org/10.1111/jfr3.12639

Del Giudice, G., Gargano, R., Rasulo, G., & Siciliano, D. (2014). Preliminary Estimate of Detention Basin Efficiency at Watershed Scale. Water Resources Management, 28(4), 897–913. https://doi.org/10.1007/s11269-014-0518-1

ERM Hong Kong. (2010). Regulation of Shenzhen River Stage 4 EIA Study: Executive Summary Report (Hong Kong Side) (p. 13). https://www.epd.gov.hk/eia/register/report/eiareport/eia_1892010/PDF/0101759_Final%20ExecSum_Combined.pdf

European Commission. Directorate General for Research and Innovation. (2015). Towards an EU research and innovation policy agenda for nature-based solutions & re-naturing cities: Final report of the Horizon 2020 expert group on 'Nature based solutions and re naturing cities' : (full version). Publications Office. https://data.europa.eu/doi/10.2777/765301

Guan, M., Sillanpää, N., & Koivusalo, H. (2015a). Storm runoff response to rainfall pattern, magnitude and urbanization in a developing urban catchment: Storm Runoff Response to Rainfall Pattern, Magnitude and Urbanization. Hydrological Processes, 30(4), 543–557. https://doi.org/10.1002/hyp.10624

Guan, M., Sillanpää, N., & Koivusalo, H. (2015b). Modelling and assessment of hydrological changes in a developing urban catchment: HYDROLOGICAL CHANGES IN A DEVELOPING URBAN CATCHMENT. Hydrological Processes, 29(13), 2880–2894. https://doi.org/10.1002/hyp.10410

Guo, K., Guan, M., & Yu, D. (2021). Urban surface water flood modelling – a comprehensive review of current models and future challenges. Hydrology and Earth System Sciences, 25(5), 2843–2860. https://doi.org/10.5194/hess-25-2843-2021

Habets, F., Molénat, J., Carluer, N., Douez, O., & Leenhardt, D. (2018). The cumulative impacts of small reservoirs on hydrology: A review. Science of The Total Environment, 643, 850–867. https://doi.org/10.1016/j.scitotenv.2018.06.188

Hallegatte, S., Green, C., Nicholls, R. J., & Corfee-Morlot, J. (2013). Future flood losses in major coastal cities. Nature Climate Change, 3(9), 802–806. https://doi.org/10.1038/nclimate1979

He, J., Qiang, Y., Luo, H., Zhou, S., & Zhang, L. (2021). A stress test of urban system flooding upon extreme rainstorms in Hong Kong. Journal of Hydrology, 597, 125713. https://doi.org/10.1016/j.jhydrol.2020.125713

Horritt, M. S., & Bates, P. D. (2001). Effects of spatial resolution on a raster based model of flood flow. Journal of Hydrology, 253(1-4), 239-249. https://doi.org/10.1016/S0022-1694(01)00490-5

Hosseinzadehtalaei, P., Tabari, H., & Willems, P. (2020). Climate change impact on short-duration extreme precipitation and intensity–duration–frequency curves over Europe. Journal of Hydrology, 590, 125249. https://doi.org/10.1016/j.jhydrol.2020.125249

IPCC. (2021). Climate Change 2021: The Physical Science Basis. Contribution of Working Group I to the Sixth Assessment Report of the Intergovernmental Panel on Climate Change [Masson-Delmotte, V., P. Zhai, A. Pirani, S.L. Connors, C. Péan, S. Berger, N. Caud, Y. Chen, L. Goldfarb, M.I. Gomis, M. Huang, K. Leitzell, E. Lonnoy, J.B.R. Matthews, T.K. Maycock, T. Waterfield, O. Yelekçi, R. Yu, and B. Zhou (eds.)].

Jarihani, A. A., Callow, J. N., McVicar, T. R., Van Niel, T. G., & Larsen, J. R. (2015). Satellite-derived Digital Elevation Model (DEM) selection, preparation and correction for hydrodynamic modelling in large, low-gradient and data-sparse catchments. Journal of Hydrology, 524, 489–506. https://doi.org/10.1016/j.jhydrol.2015.02.049

Jato-Espino, D., Sillanpää, N., Charlesworth, S. M., & Rodriguez-Hernandez, J. (2019). A simulation-optimization methodology to model urban catchments under non-stationary

extreme rainfall events. Environmental Modelling & Software, 122, 103960. https://doi.org/10.1016/j.envsoft.2017.05.008

Johnson, N. L. (1995). Continuous Univariate Distributions. 1, 769.

Lai, Y., Li, J., Gu, X., Chen, Y. D., Kong, D., Gan, T. Y., Liu, M., Li, Q., & Wu, G. (2020). Greater flood risks in response to slowdown of tropical cyclones over the coast of China. Proceedings of the National Academy of Sciences, 117(26), 14751–14755. https://doi.org/10.1073/pnas.1918987117

Lim, T. C., & Welty, C. (2017). Effects of spatial configuration of imperviousness and green infrastructure networks on hydrologic response in a residential sewershed. Water Resources Research, 53(9), 8084–8104. https://doi.org/10.1002/2017WR020631

Loperfido, J. V., Noe, G. B., Jarnagin, S. T., & Hogan, D. M. (2014). Effects of distributed and centralized stormwater best management practices and land cover on urban stream hydrology at the catchment scale. Journal of Hydrology, 519, 2584–2595. https://doi.org/10.1016/j.jhydrol.2014.07.007

Luan, B., Yin, R., Xu, P., Wang, X., Yang, X., Zhang, L., & Tang, X. (2019). Evaluating Green Stormwater Infrastructure strategies efficiencies in a rapidly urbanizing catchment using SWMM-based TOPSIS. Journal of Cleaner Production, 223, 680–691. https://doi.org/10.1016/j.jclepro.2019.03.028

Maragno, D., Gaglio, M., Robbi, M., Appiotti, F., Fano, E. A., & Gissi, E. (2018). Fine-scale analysis of urban flooding reduction from green infrastructure: An ecosystem services approach for the management of water flows. Ecological Modelling, 386, 1–10. https://doi.org/10.1016/j.ecolmodel.2018.08.002

Mård, J., Di Baldassarre, G., & Mazzoleni, M. (2018). Nighttime light data reveal how flood protection shapes human proximity to rivers. Science Advances, 4(8), eaar5779. https://doi.org/10.1126/sciadv.aar5779

Merz, B., Blöschl, G., Vorogushyn, S., Dottori, F., Aerts, J. C. J. H., Bates, P., Bertola, M., Kemter, M., Kreibich, H., Lall, U., & Macdonald, E. (2021). Causes, impacts and patterns of disastrous river floods. Nature Reviews Earth & Environment. https://doi.org/10.1038/s43017-021-00195-3

Meylan, P. (2019). Predictive hydrology. A frequency analysis approach.

Miller, A. J., Welty, C., Duncan, J. M., Baeck, M. L., & Smith, J. A. (2021). Assessing urban rainfall-runoff response to stormwater management extent. Hydrological Processes, 35(7). https://doi.org/10.1002/hyp.14287

Miller, J. D., Kim, H., Kjeldsen, T. R., Packman, J., Grebby, S., & Dearden, R. (2014). Assessing the impact of urbanization on storm runoff in a peri-urban catchment using historical change in impervious cover. Journal of Hydrology, 515, 59–70. https://doi.org/10.1016/j.jhydrol.2014.04.011

Ming, X., Liang, Q., Xia, X., Li, D., & Fowler, H. J. (2020). Real-Time Flood Forecasting Based on a High-Performance 2-D Hydrodynamic Model and Numerical Weather Predictions. Water Resources Research, 56(7). https://doi.org/10.1029/2019WR025583

Ochoa-Rodriguez, S., Wang, L.-P., Gires, A., Pina, R. D., Reinoso-Rondinel, R., Bruni, G., Ichiba, A., Gaitan, S., Cristiano, E., van Assel, J., Kroll, S., Murlà-Tuyls, D., Tisserand, B., Schertzer, D., Tchiguirinskaia, I., Onof, C., Willems, P., & ten Veldhuis, M.-C. (2015). Impact of spatial and temporal resolution of rainfall inputs on urban hydrodynamic modelling outputs: A multi-catchment investigation. Journal of Hydrology, 531, 389–407. https://doi.org/10.1016/j.jhydrol.2015.05.035

Peking University. (2016). Research Report on Comprehensive Management Plan of Shenzhen River Basin.

Qin, H., Li, Z., & Fu, G. (2013). The effects of low impact development on urban flooding under different rainfall characteristics. Journal of Environmental Management, 129, 577–585. https://doi.org/10.1016/j.jenvman.2013.08.026

Rezazadeh Helmi, N., Verbeiren, B., Mijic, A., van Griensven, A., & Bauwens, W. (2019). Developing a modeling tool to allocate Low Impact Development practices in a cost-optimized method. Journal of Hydrology, 573, 98–108. https://doi.org/10.1016/j.jhydrol.2019.03.017

Rogger, M., Agnoletti, M., Alaoui, A., Bathurst, J. C., Bodner, G., Borga, M., Chaplot, V., Gallart, F., Glatzel, G., Hall, J., Holden, J., Holko, L., Horn, R., Kiss, A., Kohnová, S., Leitinger, G., Lennartz, B., Parajka, J., Perdigão, R., … Blöschl, G. (2017). Land use change impacts on floods at the catchment scale: Challenges and opportunities for future research: LAND USE CHANGE IMPACTS ON FLOODS. Water Resources Research, 53(7), 5209–5219. https://doi.org/10.1002/2017WR020723

Ruangpan, L., Vojinovic, Z., Di Sabatino, S., Leo, L. S., Capobianco, V., Oen, A. M. P., McClain, M. E., & Lopez-Gunn, E. (2020). Nature-based solutions for hydro-meteorological risk reduction: A state-of-the-art review of the research area. Natural Hazards and Earth System Sciences, 20(1), 243–270. https://doi.org/10.5194/nhess-20-243-2020

Saksena, S., & Merwade, V. (2015). Incorporating the effect of DEM resolution and accuracy for improved flood inundation mapping. Journal of Hydrology, 530, 180–194. https://doi.org/10.1016/j.jhydrol.2015.09.069

Tellman, B., Sullivan, J. A., Kuhn, C., Kettner, A. J., Doyle, C. S., Brakenridge, G. R., Erickson, T. A., & Slayback, D. A. (2021). Satellite imaging reveals increased proportion of population exposed to floods. Nature, 596(7870), 80–86. https://doi.org/10.1038/s41586-021-03695-w

Vojinovic, Z., Alves, A., Gómez, J. P., Weesakul, S., Keerakamolchai, W., Meesuk, V., & Sanchez, A. (2021). Effectiveness of small- and large-scale Nature-Based Solutions for flood mitigation: The case of Ayutthaya, Thailand. Science of The Total Environment, 789, 147725. https://doi.org/10.1016/j.scitotenv.2021.147725

Willems, P. (2000). Compound intensity/duration/frequency-relationships of extreme precipitation for two seasons and two storm types. Journal of Hydrology, 233(1–4), 189–205. https://doi.org/10.1016/S0022-1694(00)00233-X

Wong, B. P., & Kerkez, B. (2018). Real-Time Control of Urban Headwater Catchments Through Linear Feedback: Performance, Analysis, and Site Selection. Water Resources Research, 54(10), 7309–7330. https://doi.org/10.1029/2018WR022657

Xia, X., Liang, Q., Ming, X., & Hou, J. (2017). An efficient and stable hydrodynamic model with novel source term discretization schemes for overland flow and flood simulations: NEW HYDRODYNAMIC MODEL FOR OVERLAND FLOW. Water Resources Research, 53(5), 3730–3759. https://doi.org/10.1002/2016WR020055

Yang, L., Smith, J. A., Baeck, M. L., & Zhang, Y. (2016). Flash flooding in small urban watersheds: Storm event hydrologic response. Water Resources Research, 52(6), 4571–4589. https://doi.org/10.1002/2015WR018326

Yang, Q., Shao, J., Scholz, M., & Plant, C. (2011). Feature selection methods for characterizing and classifying adaptive Sustainable Flood Retention Basins. Water Research, 45(3), 993–1004. https://doi.org/10.1016/j.watres.2010.10.006

Zeiger, S. J., & Hubbart, J. A. (2021). Measuring and modeling event-based environmental flows: An assessment of HEC-RAS 2D rain-on-grid simulations. Journal of Environmental Management, 285, 112125. https://doi.org/10.1016/j.jenvman.2021.112125

Zellner, M., Massey, D., Minor, E., & Gonzalez-Meler, M. (2016). Exploring the effects of green infrastructure placement on neighborhood-level flooding via spatially explicit simulations. Computers, Environment and Urban Systems, 59, 116–128. https://doi.org/10.1016/j.compenvurbsys.2016.04.008

Zhu, Z., Wright, D. B., & Yu, G. (2018). The Impact of Rainfall Space-Time Structure in Flood Frequency Analysis. Water Resources Research, 54(11), 8983–8998. https://doi.org/10.1029/2018WR023550